



Nano-newton scale hydrodynamic force measurement through CFD modeling of spinning disc

Intizar Ali^{1*}, Zarah Walsh Korb², Tanweer Hussain³, Abi Waqas⁴, Inam Ul Ahad¹

¹I-Form, SFI Research Centre for Advanced Manufacturing, School of Mechanical & Manufacturing Engineering, Dublin City University, Dublin, Ireland

²Department of Chemistry, University of Basel, Mattenstrasse 22, 4058 Basel, Switzerland

³Department of Mechanical Engineering, Mehran UET Jamshoro Sindh, Pakistan

⁴Department of Telecommunication, Mehran UET Jamshoro Sindh, Pakistan

Intizar.ali@dcu.ie

Abstract. Understanding the molecular scale and mesoscale behavior of cell adhesion proteins is highly useful in solving real-world tissue engineering problems. Therefore, the present study attempts to analyze the mesoscale behavior of adhesions through numerical simulation. The computational fluid dynamics CFD simulation is performed to determine the hydrodynamic force on the mesoscale using spherical particles that represent the cells, attached to a spinning disc through the force of adhesion. The spinning disc is rotating in a TBS buffer with 1 mM of Ca²⁺ with almost similar physical properties to water. To determine the Nano-newton scale force eight spherical particles were attached to the spinning disc along the radial direction. The hydrodynamic force acts on the mesoscale spherical particles were determined at 3000 and 4000 rpm. As the size of the particles is negligible as compared to the size of the spinning disc and the Reynolds number is quite low, therefore, flow is considered as laminar. Numerical simulation revealed that hydrodynamic force acting on the spherical particles varies linearly along the radial direction. Moreover, fluid velocity over the disc surface also varies linearly in the radial direction. It is also estimated that drag force acting the particles is 10 times higher as compared to lift force and force acting in radial direction.

1 Introduction

Adhesion plays an integral role in cell communication and regulation and is of fundamental importance in the development and maintenance of tissues. The ability of a single cells to adhere to an extracellular matrix (ECM) or another cell is known as cell adhesion. It is important to understand how cells communicate and coordinate with one another in multicellular organisms. Most mammalian cells are anchorage-dependent and adhere strongly to the substrate in vitro [1]. A cell's surface has more chemical bonds when it adheres to other things, according to the "cell adhesion model"[2, 3].

Signals that control cell motility, adhesion, differentiation, and cycle are stimulated by cell adhesion [4]. One of the most important factors in the design and development of biomaterials is the cellular affinity for the substrate. Cell adhesion plays a crucial role in the formation and upkeep of tissues and is also necessary for cell communication and regulation. Numerous illnesses, such as osteoporosis [5], cancer [6], atherosclerosis [7, 8], arthritis [9], and changes in cell adhesion, can be identified by changes in this distinguishing factor.

Cell behaviour and function are subject to the mechanical interactions that exist between a cell and its extracellular matrix (ECM). The growing significance of cell mechanobiology in physiology and illness, together with its indispensable role, has sparked intense interest in devising techniques to quantify the mechanical characteristics of cells. Studies on cell adhesion can often be divided into two categories: cell attachment and cell dissociation events. Many methods have been developed to study both single cells and cell populations in order to analyse cell adhesion events. Cell adhesion attachment events centre on the process by which cells adhere to the substrate, whereas cell adhesion detachment events entail applying load to cause the attached cells on the substrate to separate as shown in Fig. 1.

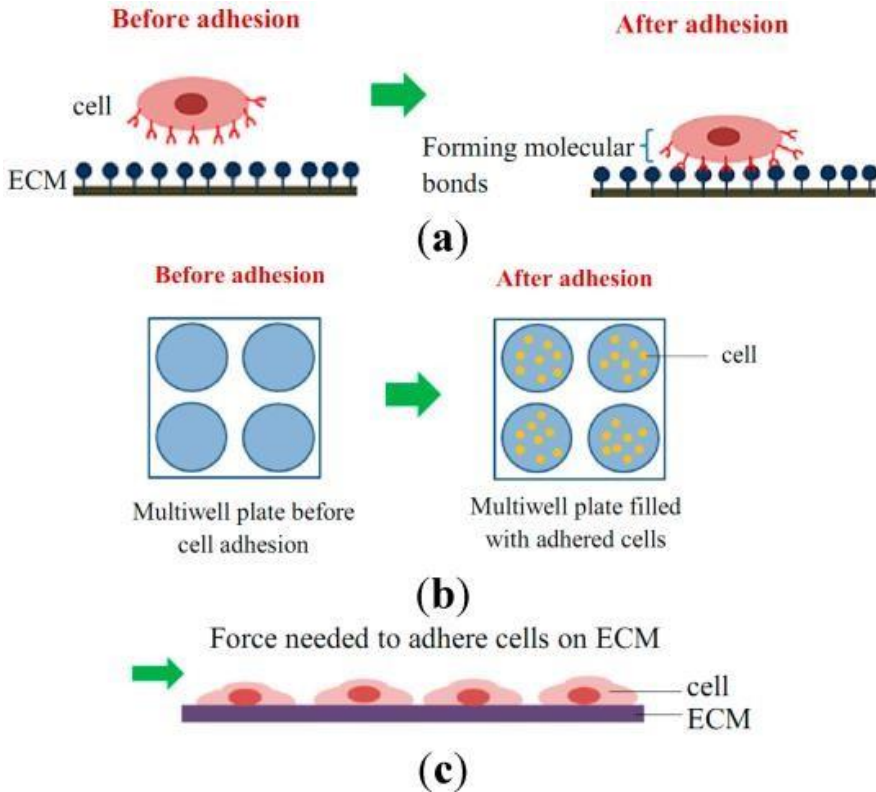


Fig. 1. shows a schematic diagram of the cell adhesion attachment events for the following three types of research: (a) single cell studies using molecular bond formation; (b) cell population studies using static adhesion (like the wash assay technique); and (c) cell population studies using dynamic adhesion (like the microfluidic technique, spinning disc).

Shear stress produced by a rotating disc device is used in the spinning disc technique. On a circular glass coverslip or the surface of a disc, cells are initially seeded (usual diameter 10–50 mm). Afterwards, these discs are fastened to a revolving apparatus that is positioned inside a buffer solution-filled chamber [10, 11]. The rotating tool may rotate between 100 and 4000 revolutions per minute. The adherent fractions of cells are often counted manually [12] or automatically using image processing software [13], together with optical microscopy to determine the number of cells before and after spinning. The present study aims to understand cell detachment dynamics over the spinning disc.

2 Numerical modeling

2.1 Problem definition & Modeling

To understand cell detachment and measure the hydrodynamic force acting on the spherical particles on the mesoscale, i.e., the cell population, the spinning disc method has been widely applied over the last decade. For, that purpose, a Computer Added Design (CAD) model of the spinning disc is developed in ANSYS Design Modeller, then the 5 μm spherical particles were attached to the disc along the radial direction at equal distance, one particle is also attached at centre of the spinning disc. Four rows of particles were attached to the disc along positive and negative horizontal and vertical axis. Then the cylindrical fluid domain is created around the spinning disc and the solid body is removed from the fluid domain. The CAD model of the computational domain is presented in Fig.2 (a). The design parameters of the spinning disc and the fluid domain are presented in Table: 1.

Table. 01. Design specification of the spinning disc and spherical particle

Parameter	Values
Spinning Disc diameter	500 μm
Spinning Disc thickness	20 μm
Particle diameter	5 μm
Particle embedded in disc	0.3 μm
Fluid domain diameter	700 μm
Fluid domain depth	420 μm
Particle to particle distance	30 μm

2.2 Meshing and CFD modeling

Once the fluid domain is generated the, the domain is discretized into small control volumes to solve the Reynolds Averaging Navier-Stokes (RANS) equations through the finite volume method. The tetrahedral mesh elements were used to generate the mesh, where a non-uniform mesh is generated through refining the element size at the disc. The element size over the disc surface is 2 μm , whereas the element size at the spherical particles is 2 μm . The meshing in the curvature and proximity region were further refined. Later, names were assigned to the face of the computational domain and numbers were assigned to spheres, e.g., the sphere at the centre is numbered as sphere_0 and the sphere adjacent to central sphere is named as sphere_1 and in this way spherical particles were numbered from the center to the edge of the spinning disc along the radial path. Then CFD modeling is carried out where steady state simulation is performed by using a pressure-based solver and water with a density of 998.5 kg/m^3 and viscosity of 0.001 Pa is used. Flow is considered as laminar, which significantly reduced computational cost and time. The moving frame of reference is used to introduce the angular speed to the spinning disc.

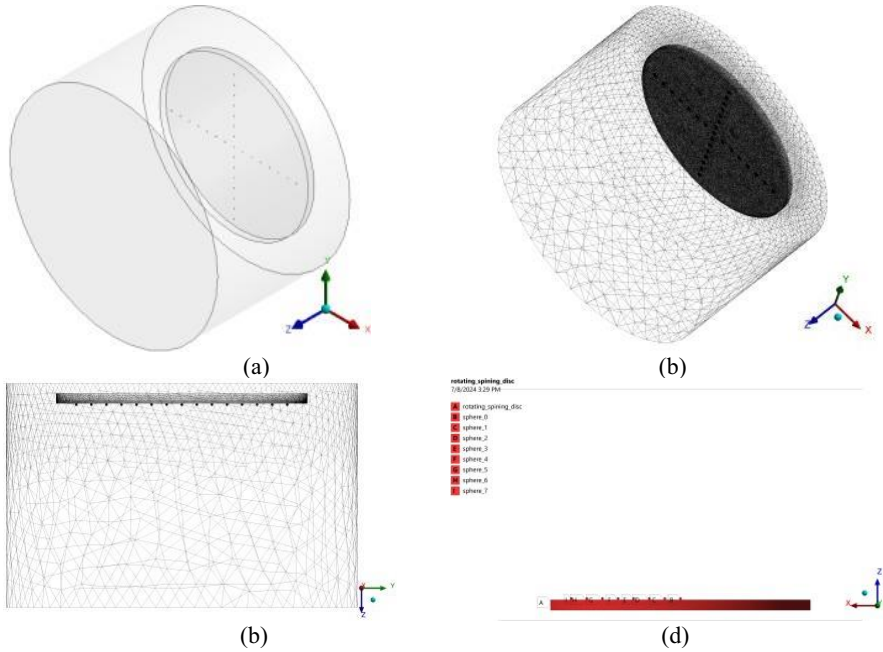


Fig. 2 (a) 3-dimensional CAD model of the spinning disc with spherical particles attached on it and the fluid domain, (b) isometric view of the meshed model of the computational domain showing refined mesh of the spinning disc, (c) side view of the fluid domain containing spinning disc and particles, and (d) named sections of computational domain and spherical particles were number liked sphere_0 showing particle at centre, sphere_1 particle adjacent central sphere and so on.

3 Results & discussion

3.1 Forces acting on the particles

The hydrodynamic forces, i.e., lift and drag forces experienced by the spherical particle attached to spinning disc at different rotational speed values is plotted and presented in Fig. 3. From the graph it can be observed that drag force acting on the particles is significantly higher compared to lift forces. It is also observed that the rotational speed of the spinning disc has a considerable impact on the drag force acting on the spherical particles. Moreover, the graph also shows that drag force has an almost linear relationship with radial position and that the drag force is about zero at the central particle and increases with radial distance, such that the last particle near the edge of disc experiences the highest drag force. It is also noted that rotational speed has negligible impact on the magnitude of lift force acting on the particle.

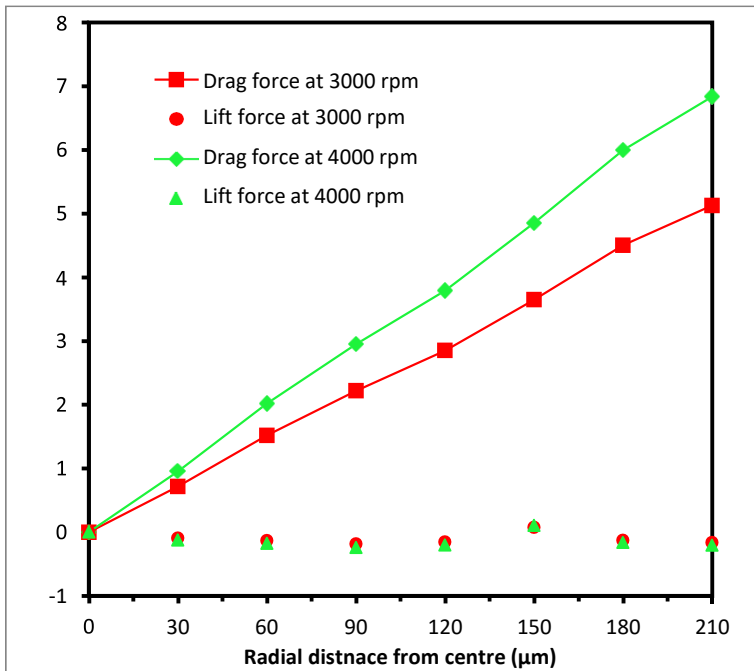


Fig. 3 The hydrodynamic forces (lift and drag force) acting on the spherical particle location at different positions along the radial path on the disc surface. The lift and drag force at two different angular speed of the spinning disc, the particles from the surface detached at point where lift or drag force value exceeds the adhesion force on the particle.

3.2 Flow analysis over rotating disc with small particles

In this section, velocity and wall shear stress distribution over the spinning disc is discussed and presented in Fig. 4(a-d) at different angular speed values. From the tangential fluid velocity variation over the disc surface, it is noted that the maximum tangential velocity value increases with an increase in rotational rate of spinning disc. It is also observed that tangential velocity increases along the radial direction, as a result of this drag acting on particles also increases along the radial direction. The velocity contour also highlights that there is a ring-like structure having specific radial thickness where tangential velocity remains constant in that portion. The wall shear stress distribution over the disc surface shows that the magnitude of shear stresses is quite low over the surface of spinning except in regions below the spherical particles. From the wall shear stress contour, it is clear that shear stress reaches a maximum value of 880 Pa at the rotational speed of 4000 rpm. Moreover, it is further clear from WSS contours that when the WSS limit is varied i.e., from 100-880 Pa, only the region below the spheres were highlighted showing that WSS are high only in region contact of spherical particles with disc, thus wall shear is quite low at spinning disc.

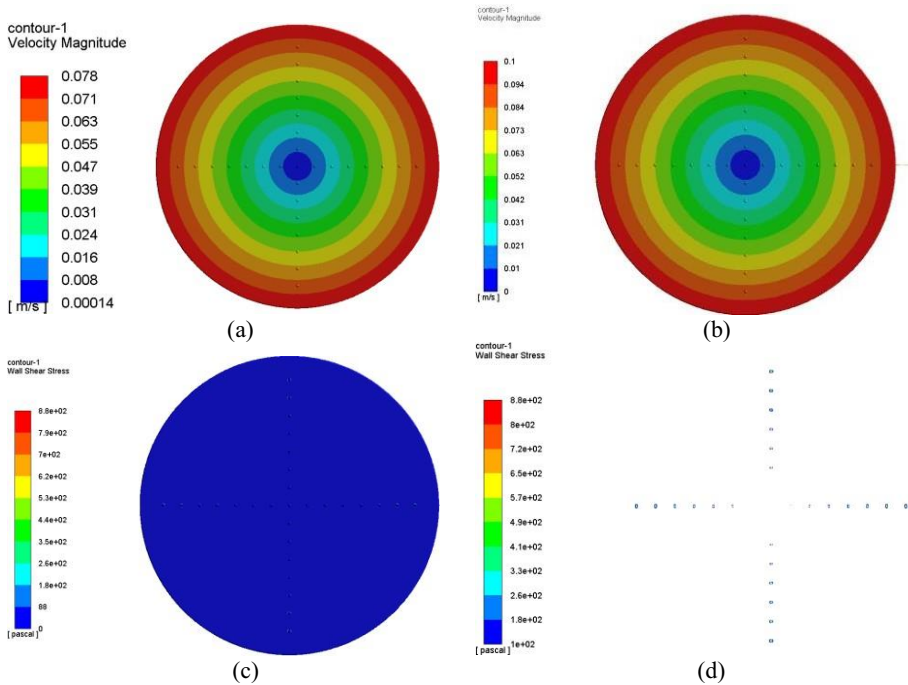


Fig. 4 Fluid velocity distribution over disc with spherical particles attached to it for different angular speed values (a) 3000 rpm (b) 4000 rpm (c) Overall wall shear distribution over the disc ranging from 0-880 Pa, (d) wall shear stress on disc ranging from 100-880 Pa showing region of disc have wall shear within this range, it is clear that wall shear over disc surface is quite low and wall shear is high in the region beneath spheres.

4 Conclusion

This research work aims; at analyzing the mesoscale behavior of cell adhesion through CFD simulation. The CFD simulation is performed to determine the hydrodynamic force on the mesoscale spherical particles attached to the spinning disc through the force of adhesion. Effect of disc spinning speed is analyzed on the hydrodynamic force and wall shear stresses acting on the particles. Numerical simulation revealed that hydrodynamic force acting on the spherical particles varies linearly along the radial direction. It is also found that disc spinning speed has significant impact on the hydrodynamic forces. Moreover, fluid velocity over the disc surface also varies linearly in the radial direction. It is also estimated that drag force acting the particles is 10 times higher as compared to lift force and force acting in radial direction. It is also noticed that wall shear over disc surface is quite low and wall shear is high in the region of disc beneath spheres particles.

References

1. G. Sagvolden, I. Giaever, E. Pettersen, and J. Feder, "Cell adhesion force microscopy," *Proceedings of the National Academy of Sciences*, vol. 96, pp. 471- 476, 1999.
2. M. Dembo, D. Torney, K. Saxman, and D. Hammer, "The reaction-limited kinetics of membrane-to-surface adhesion and detachment," *Proceedings of the Royal Society of London. Series B. Biological Sciences*, vol. 234, pp. 55-83, 1988.

3. Y. Shen, M. Nakajima, S. Kojima, M. Homma, M. Kojima, and T. Fukuda, "Single cell adhesion force measurement for cell viability identification using an AFM cantilever-based micro putter," *Measurement science and technology*, vol. 22, p. 115802, 2011.
4. S. Huang and D. E. Ingber, "The structural and mechanical complexity of cell- growth control," *Nature cell biology*, vol. 1, pp. E131-E138, 1999.
5. P. Cho, G. B. Schneider, B. Kellogg, R. Zaharias, and J. C. Keller, "Effect of glucocorticoid-induced osteoporotic-like conditions on osteoblast cell attachment to implant surface microtopographies," *Implant dentistry*, vol. 15, pp. 377-385, 2006.
6. T. Okegawa, R.-C. Pong, Y. Li, and J.-T. Hsieh, "The role of cell adhesion molecule in cancer progression and its application in cancer therapy," *Acta Biochimica Polonica*, vol. 51, pp. 445-457, 2004.
7. C. N. Serhan and J. Savill, "Resolution of inflammation: the beginning programs the end," *Nature immunology*, vol. 6, pp. 1191-1197, 2005.
8. S. I. Simon and C. E. Green, "Molecular mechanics and dynamics of leukocyte recruitment during inflammation," *Annu. Rev. Biomed. Eng.*, vol. 7, pp. 151-185, 2005.
9. Z. Szekanecz and A. E. Koch, "Endothelial cells and immune cell migration," *Arthritis Research & Therapy*, vol. 2, pp. 1-6, 2000.
10. K. V. Christ and K. T. Turner, "Methods to measure the strength of cell adhesion to substrates," *Journal of Adhesion Science and Technology*, vol. 24, pp. 2027-2058, 2010.
11. C. Reutelingsperger, R. Van Gool, V. Heijnen, P. Frederik, and T. Lindhout, "The rotating disc as a device to study the adhesive properties of endothelial cells under differential shear stresses," *Journal of Materials Science: Materials in Medicine*, vol. 5, pp. 361-367, 1994.
12. N. D. Gallant, K. E. Michael, and A. J. Garcia, "Cell adhesion strengthening: contributions of adhesive area, integrin binding, and focal adhesion assembly," *Molecular biology of the cell*, vol. 16, pp. 4329-4340, 2005.
13. J. García, P. Ducheyne, and D. Boettiger, "Quantification of cell adhesion using a spinning disc device and application to surface-reactive materials," *Biomaterials*, vol. 18, pp. 1091-1098, 1997.

Open Access This chapter is licensed under the terms of the Creative Commons Attribution-NonCommercial 4.0 International License (<http://creativecommons.org/licenses/by-nc/4.0/>), which permits any noncommercial use, sharing, adaptation, distribution and reproduction in any medium or format, as long as you give appropriate credit to the original author(s) and the source, provide a link to the Creative Commons license and indicate if changes were made.

The images or other third party material in this chapter are included in the chapter's Creative Commons license, unless indicated otherwise in a credit line to the material. If material is not included in the chapter's Creative Commons license and your intended use is not permitted by statutory regulation or exceeds the permitted use, you will need to obtain permission directly from the copyright holder.

